Finite element model updating of a plate type structure made of composite material using a network of PZT

Finite element model updating of a plate type structure made of composite material using a network of PZT

M A M Salem[1], M Kassem[2], M S Amin[3*], H M Farag[4] and A Osman[5].

[1]Department of Civil Engineering, Military Technical College.
[2]Department of Aircraft Mechanics, Military Technical College.
[3]Department of Civil Engineering, Military Technical College.
[4]Department of Civil Engineering, Military Technical College.
[5]Department of Civil Engineering, Military Technical College, Cairo, Egypt.

[*]Corresponding author E-mail: melbeblawy@mtc.edu.eg

Abstract. Ambient vibrations are one of the most unpredicted, undesired, and uncontrolled destructive causes of sudden failure for many types of structural systems, predominantly those made of FRP thin plates. FRP thin plates may undergo dramatic collapse beneath the periodic ambient loads associated with frequencies, particularly those approaching natural frequencies. Much research has been done over the last few decades to enhance the structural damping behaviour capabilities of thin plates against ambient vibrations via several means and systems of active vibration control. Recent, exceptional advancements in the field of smart materials and their applications in the field of active vibration control have provided a viable alternative to conventional vibration control tools (sensors/actuators). For instance, the coupled properties inherited by PWAS were utilised to develop durable, compact, and efficient actuators/sensors. To minimize the influence of the disparity between the theoretical and actual dynamic structure performances, the numerical FEM has to be updated using real structural data. In the present study, a model update of the structural parameters of a smart beam is carried out by employing PWAS as smart vibration control tools (sensor/actuator) that have been previously installed on the substrate structure. A finite element model is developed to mimic this intelligent beam. Then, laboratory experiments are undertaken to determine system parameters, which are used to update the finite element model. Finally, optimization is done to minimize the FEM variance in the designated structure vibration response from the real one.

1.Introduction

Over the course of the past few decades, smart/adaptive structures have been designed to serve as useful components for a wide variety of contemporary structural systems. In today's world, the uses of these technologies are not just limited to high-tech systems like aircraft or spacecraft; rather, they have proliferated to become a part of many aspects of our day-to-day lives, including things like vehicles, infrastructure, building management systems (BMS), etc.

There are many definitions that relay on the qualities, functionality, and components of smart structures. One of the most traditional definitions of them classified them as structure components with sensors and actuators embedded or attached in/to them. Since these actuators / sensors are functioning

through a coordinated control system, the structural component is capable of responding remotely and simultaneously to any external stimuli, giving the desired designated react for such stimuli [1].

The preceding definition makes it abundantly clear that the primary characteristic of smart structures is an organized interaction between mechanical and electronic components that results in elasto-mechanical structural qualities. This is the defining element of a smart structure. In addition, the primary functions that should be targeted by smart structures can be summed up as structural health monitoring (SHM), active vibration control, active shape control, and active noise control. For any of these functions to work as intended, the primary components that are required are the following: structure, sensors, actuators, and a control system [2, 3].

The application of smart materials for the purpose of improving the functionality of smart structures opened up a new horizon for such systems. This new horizon is referred to as the unique coupled abilities of smart materials, which improved the functionality of smart structure systems by making them lighter and more operational. Piezoelectric material is one of the most well-known examples of a smart material whose advancement in recent years has been so spectacular. Among the shapes that this smart material can take, for example, are ceramics (PZT) or polymers.

This type of material enables an appropriate alternative to permanently insert a very little and inexpensive piece of material within the structure, which lasts for the entirety of the structure's operating life time and provides sustained stimulation for the substrate structure [1]. Piezoelectric wafer active sensor (PWAS) has received attention owing to its electro-mechanical coupling, which qualifies it to be a simultaneous energy transducer from mechanical to electrical energy and vice versa. As a result, it can operate as both a sensor and an actuator.

Particularly for structures in a working environment with noticeable ambient vibrations, vibration control is a critical issue that can prevent a wide range of problems, from minor malfunctions and inappropriate structural performance to catastrophic failures and even disasters [4]. When studying the destructive behavior of structures even under low amplitude cyclic loads, many researchers have implied vibration control systems in which integrated actuators excite all structural modes of interest [5]. Because of the myriad advantages piezoelectric ceramic offers, it quickly became one of the most widely used smart materials in this area [6]. Vibrations in cantilevered structures [7-10], frame structures [11], and plate structures [12, 13] were all managed with the help of PWASs. Therefore, the use of PWASs' actuators will be compatible with the integration of vibration control systems using the same actuating set simultaneously for thin walled structures.

Updating the model of the numerically simulated system is essential for building a high-quality vibration control system. This will allow for a more precise prediction of the system's behavior in response to operating vibrations from outside sources. Numerous academics have created many techniques and processes in recent years to assess the structural parameter variation between final form counterparts and numerically calculated ones.

To improve a finite element model (FEM) of a flat plate wing construction with a shaker and a laser doppler vibrometer, Levin and Lieven [14] created a blended simulated annealing (BSA) technique using a standard genetic algorithm (GA). Using vibration data collected with an impact hummer and accelerometer, Wang et al. [15] incorporated an acceleration frequency response function (FRF) into the optimization process for a honey comb sandwich beam FEM update. Orthotropic fiber reinforced polymer (FRP) substrate structures have been simulated numerically using ABAQUS software by Mishra et al. [16] for a 2 meter span I beam and by Mondal and Chakraborty [17] for a 30x40x1 cm plate of FRP. For both structures, the sensitivity based inverse approach offered by the implemented FE software was carried out to estimate elastic material parameters, which were set to be updating parameters within the 1st four natural modes. Shah et al. [18] improved the accuracy of the dynamic behavior prediction for a 2-mm-thick carbon fiber reinforced epoxy (CFRE) plate by reducing the total error of the 1st ten modes from 42.61 percent to 25.05 percent by applying FEM updating for Young's modulus, shear modulus, Poisson's ratio, and density as potential updating parameters using Nastran SOL 200 software analysis capabilities. Also, Bahari et al. [19] employed modal-based updating

methods with NASTRAN SOL 200 to successfully apply a FEM update to a thin cold-rolled mild steel plate, where the overall error of the initial FEM of the plate was reduced from 45.12 percent to 6.28 percent. Bolted structures model update was brought to spot by correlating FEM to experimental modal analysis (EMA) and manipulating bolts material properties in order to enhance the dynamic behavior of bolted joints [20, 21].

The structural parameters of the numerical FEM of any substrate structure that undergoes vibration control system have to be updated with real structural data in order to reduce the impact of the gap in performance that exists between the numerical and actual dynamic structure performances. Fortunately, the permanently installed PZT sensors and actuators could be used as sufficient model update tools. In this study, a model update of the structural parameters of a smart beam is carried out by utilizing vibration control smart tools (sensor/actuator PWAS) that have previously been installed on the substrate structure. A model based on finite elements is created to simulate a smart beam equipped with two PWASs acting as sensor and actuator. The next step is to conduct tests in a laboratory in order to identify the structural system parameters, which are then used to update the finite element model. Finally, an optimization procedure is carried out in order to decrease the variance between the FEM-defined structure's vibration response and the real one.

2. piezo ceramics

Piezoelectric material is one of the most widely used active smart materials, which can be defined as a material with the ability to change its geometric or material properties in response to the application of electric, thermal, or magnetic fields, thereby acquiring an inherent capacity to transduce energy [22]. The unique coupling attribute of piezoelectricity enables PWASs to function as bidirectional electromechanical energy transducers shown in figure1. Thus, PWAS can alternately serves as a sensor or an actuator.

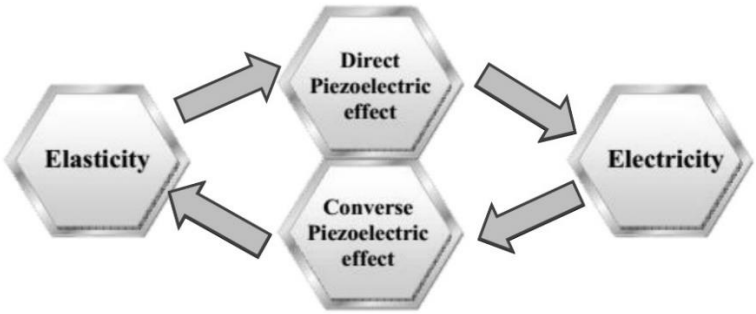

Figure 1. Direct effect and converse effect of PWAS

Based on the fundamental laws of thermodynamics, the IEEE Piezoelectric Standards [22, 23] developed constitutive equations of linear piezoelectricity. Ikeda [24] then expanded these formulas into four primary forms of 3D, the most popular of which is the stress-charge form utilized in piezoelectric analysis , shown in equation (1)

$$\begin{bmatrix}\{T\}\\ \{D\}\end{bmatrix}=\begin{bmatrix}[c^E] & -[e]^T\\ [e] & [\varepsilon^S]\end{bmatrix}\begin{bmatrix}\{S\}\\ \{E\}\end{bmatrix} \quad (1)$$

where $\{T\}$ is the stress vector, $\{D\}$ is the electric displacement, $[c^E]$ is piezoelectric material stiffness matrix at fixed field, $[e]$ is piezoelectric constant stress matrix, $[\varepsilon^S]$ is the orthogonal permittivity at fixed strain, $\{S\}$ the strain vector, and $\{E\}$ is electric field vector.

This formula can be then expanded to the next two equations (2,3)

$$\begin{bmatrix}T_1\\ T_2\\ T_3\\ T_4\\ T_5\\ T_6\end{bmatrix}=\begin{bmatrix}c_{11}^E & c_{12}^E & c_{13}^E & 0 & 0 & 0\\ c_{12}^E & c_{11}^E & c_{13}^E & 0 & 0 & 0\\ c_{13}^E & c_{13}^E & c_{33}^E & 0 & 0 & 0\\ 0 & 0 & 0 & c_{44}^E & 0 & 0\\ 0 & 0 & 0 & 0 & c_{44}^E & 0\\ 0 & 0 & 0 & 0 & 0 & c_{66}^E\end{bmatrix}\begin{bmatrix}S_1\\ S_2\\ S_3\\ S_4\\ S_5\\ S_6\end{bmatrix}-\begin{bmatrix}0 & 0 & e_{31}\\ 0 & 0 & e_{31}\\ 0 & 0 & e_{33}\\ 0 & e_{15} & 0\\ e_{15} & 0 & 0\\ 0 & 0 & 0\end{bmatrix}\begin{bmatrix}E_1\\ E_2\\ E_3\end{bmatrix} \quad (2)$$

$$\begin{bmatrix}D_1\\ D_2\\ D_3\end{bmatrix}=\begin{bmatrix}0 & 0 & 0 & 0 & e_{15} & 0\\ 0 & 0 & 0 & e_{15} & 0 & 0\\ e_{31} & e_{31} & e_{33} & 0 & 0 & 0\end{bmatrix}\begin{bmatrix}S_1\\ S_2\\ S_3\\ S_4\\ S_5\\ S_6\end{bmatrix}+\begin{bmatrix}\varepsilon_{11}^S & 0 & 0\\ 0 & \varepsilon_{11}^S & 0\\ 0 & 0 & \varepsilon_{33}^S\end{bmatrix}\begin{bmatrix}E_1\\ E_2\\ E_3\end{bmatrix} \quad (3)$$

In this context, equation (2) explains the behavior of the actuator, while equation (3) describes the sensing action that can be carried out by PWAS. In the current investigation, APC850, two 1x1 cm PZT ceramics with a thickness of 0.35 mm and the properties shown in table (2) are used to equip the specimen smart beam. One of these ceramics functions as an actuator, and the other is used as a sensor.

3. Finite model design

The test specimen is two layers cantilever beam of Epoxy Carbon Woven (ECW) (230 GPa) Wet [25] at 0° orientation angel with the structural properties shown in table (1). This specimen is equipped at its surface with two PWASs of APC850 PZT material [26] with coupled electromechanical properties shown in table (2).

Table 1 Epoxy Carbon Woven (230 GPa) Wet[25]

Properties	ECW-230
E_x, E_y	59.16 GPa
E_z	7.5 GPa
G_{xz}, G_{yz}	2.7 GPa
G_{xy}	1.7 GPa
ν_{xz}, ν_{yz}	0.3
ν_{xy}	0.04
ρ_s	1451 kg/m^3

Where $E_x, E_y,$ and E_z denote Young's moduli in the X, Y, and Z directions, G is the shear modulus, ν is the Poisson ratio, and ρ is the mass density.

A relatively small sized specimen with the dimensions shown in figure 2 is selected in order to prove the presented concept, with thicknesses of 0.4 mm and 0.35 mm for the ECW beam and PWASs respectively, where PWAS (1) acts as an actuator and PWAS (2) acts as a sensor.

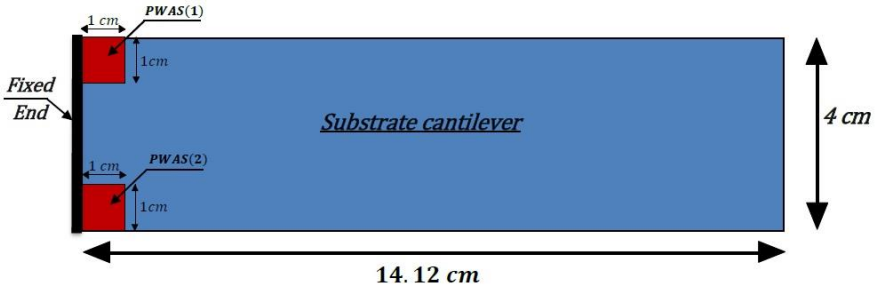

Figure 2. Test article configuration

Table 2 Properties of APC850 material[26]

Properties	APC850
E_x, E_y	63.24 GPa
E_z	54.00 GPa
G_{xz}, G_{yz}	22.00 GPa
G_{xy}	24.00 GPa
ν_{xz}, ν_{yz}	0.41
ν_{xy}	0.3
ρ_z	7600 kg/m^3
ε_x^T	1.734×10-8 F/m
ε_z^T	1.682×10-8 F/m
e_{31}	-5.35 C/M^2

The finite element model of the presented specimen was created with the help of ANSYS 22R1 software. The PWAS locations are selected to introduce the maximum available strains of the substrate cantilever for the all first 10 modes, which, according to equations (2,3), will provide the best stimulation and sensing capabilities for the two PWASs while acting as actuators or sensors. Salem [27] highlighted differences in the choices of solid element and shell element for such a dynamic analysis of thin plate, where shell element exhibited more relabel behavior. As a result, modelling the substrate cantilever beam requires the employment of a quadratic shell element. whereas the coupled characteristic of the PWASs is mimicked by employing 226 solid elements, which is offered by the software for this purpose. According to Makkonen et al. [28], the substrate cantilever and PWASs finite element size are assigned to be 2 mm. Because the dynamic analysis is only performed in the first 10 modes (less than 100 KHz), the thickness of the adhesive layer is ignored in the FEM. This is because the effect of the adhesive layer is not noticeable at such low frequencies [27, 29]. The model depicted in its discretized form can be seen in figure 3.

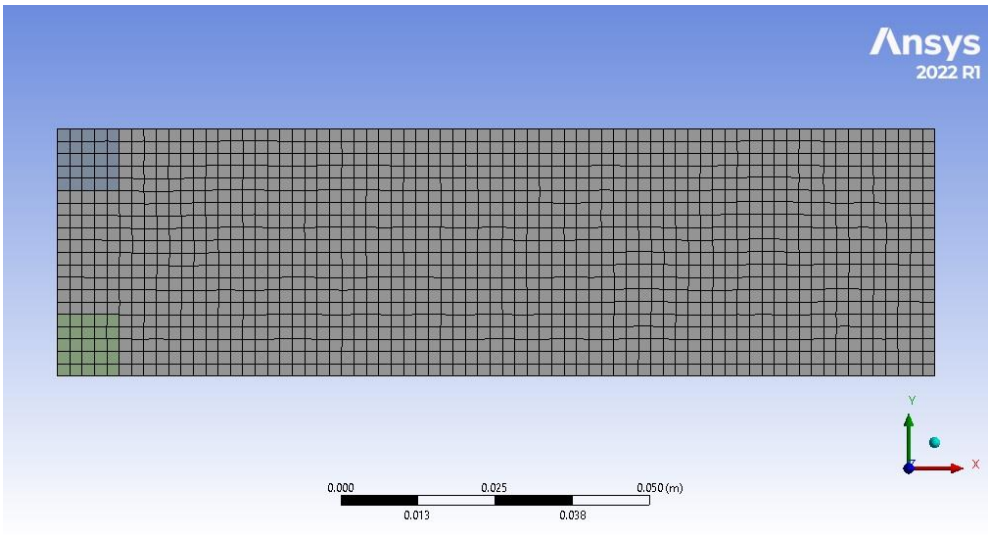

Figure 3. FEM of the test article

Modal analysis is run for the simulated FEM for the 1st 10 natural modes, the results are illustrated in figure 4 and summarized in table (3)

Table 3 Natural mode shapes frequencies of FEM

Mode number	Frequency(Hz)	Description
1	22.63	1st bending
2	139.55	1st torsion
3	140.71	2nd bending
4	390.71	3rd bending
5	436.42	2nd torsion
6	757.85	4th bending
7	782.81	3rd torsion
8	1201.8	4th torsion
9	1236.9	5th bending
10	1661.4	1st bending @ X axis

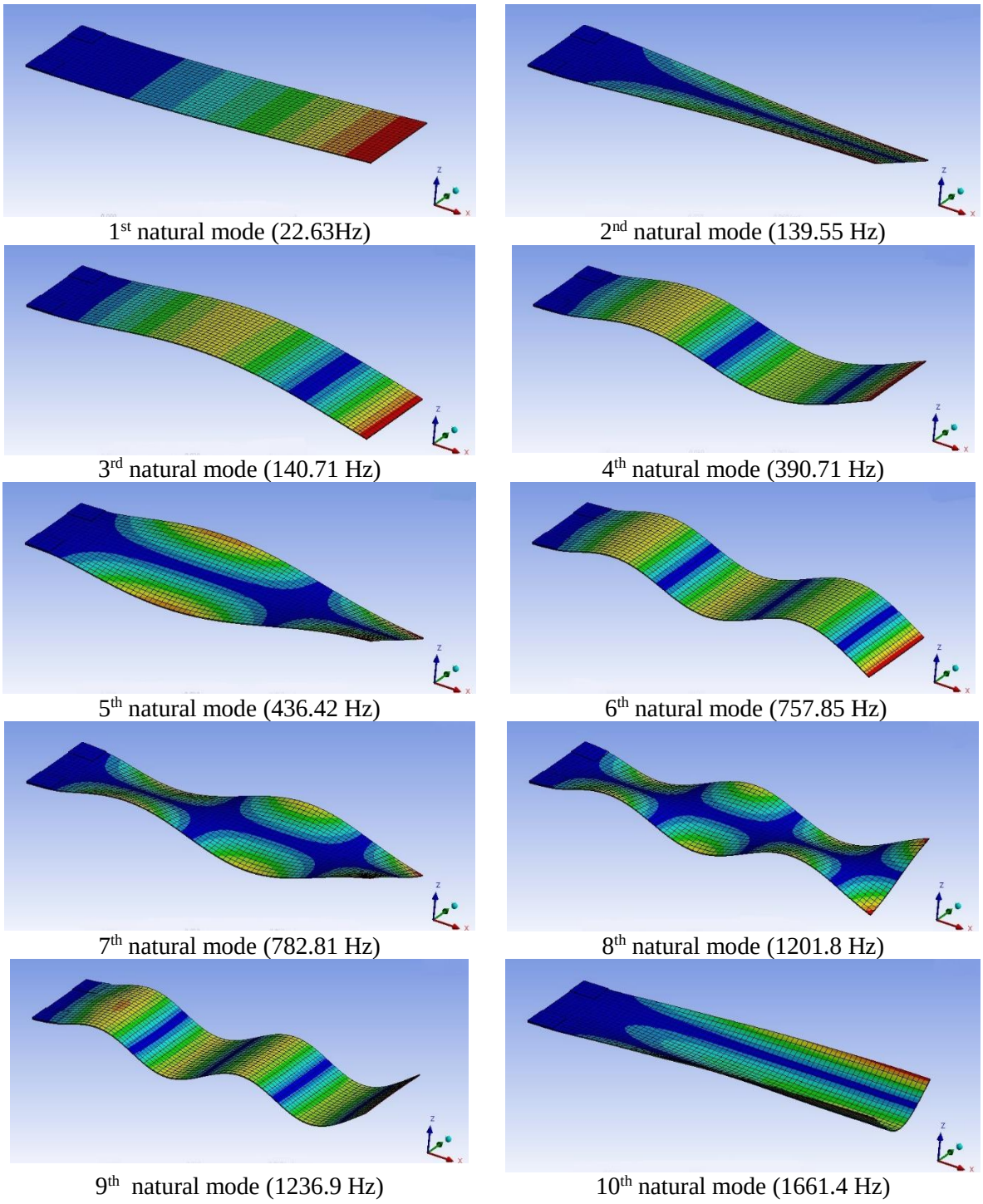

Figure 4. FEM natural modes of simulated test article

The selection of effective modes to be set as datum for FEM update is based on the effective mass fraction shown in table (4)

Table 4 Effective Mass percentages of natural modes

Mode number	Effective mass (%)					
	X direction	Y direction	Z direction	Rot X direction	Rot Y direction	Rot Z direction
1	0.23E-6	0.55E-11	**50.6**	37E-2	**95.9**	0.15E-7
2	0.76E-10	0.51E-3	0.27E-3	**15.2**	0.61E-4	0.78E-3
3	0.87E-5	0.14E-7	**16.1**	**11.9**	**3.2**	0.77E-6
4	0.65E-4	0.31E-8	6.1	**4.5**	0.52	0.43E-5
5	0.27E-9	0.60E-2	0.20E-5	2	0.54E-7	0.92E-2
6	0.23E-3	0.31E-6	**3.8**	**2.76**	0.17	0.20E-4
7	0.81E-10	0.03	0.17E-4	1	0.91E-6	0.04
8	0.80E-8	0.14	0.88E-5	0.79	0.17E-6	0.22
9	0.54E-3	0.21E-6	**3**	**2.1**	0.08	0.27E-4
10	0.36E-5	0.44E-4	0.31E-2	0.18E-2	0.81E-4	0.64E-4

4. Laboratory setup

The used PWASs are selected to have wrap-around electrode pattern where the two electrodes are on the same surface. Then, the electrodes are tin soldered at temperature 175 C° which is less than half of cure point temperature for APC 850 [26] as shown in figure 5. The test article is prepared as shown in figure 6, LOCTITE EA 9462 [30] epoxy is used as an adhesive material to attach the piezo-ceramic actuator and sensor to the cantilever beam surface with an ultimate shear strength up to 2.8 MPa. The smart beam is then fixed at the end using two clamps with four bolts and nuts.

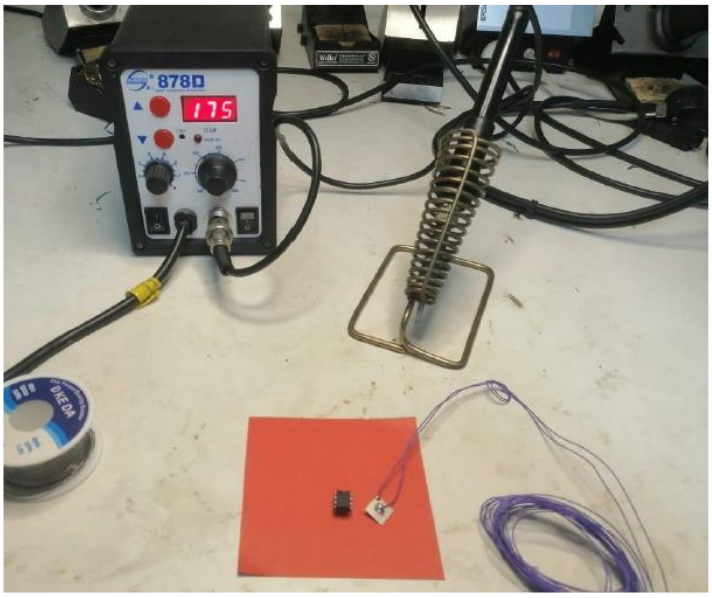

Figure 5. soldering process of PWAS.

An electric signal is induced using a Rigol DG 4062 function generator to stimulate smart beam response in the desired frequency range at a sampling rate of 1 KHz; the signal is then amplified to 50

volts, which is the safe operating voltage of the used PWAS to avoid depolarization [26]. the amplified signal is used to stimulate PWAS number (1) which act as an actuator. Using the charge amplification circuit shown in figure 7, the response of PWAS (2), which acts as a sensor, is amplified and then received at National Instruments BNC_2110 data acquisition. The final output signal is processed using LabVIEW software and then Fourier transform to get the spectrum of the frequency response function (FRF). The schematic of the test is shown in figure 8.

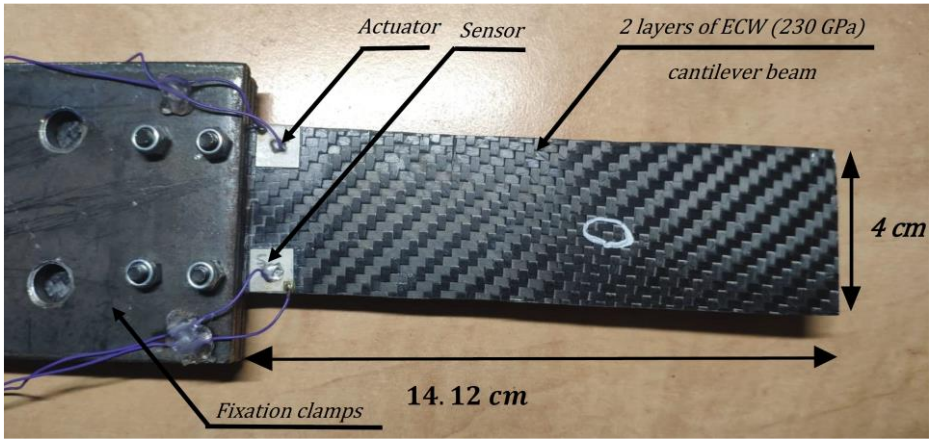

Figure 6. laboratory specimen setting.

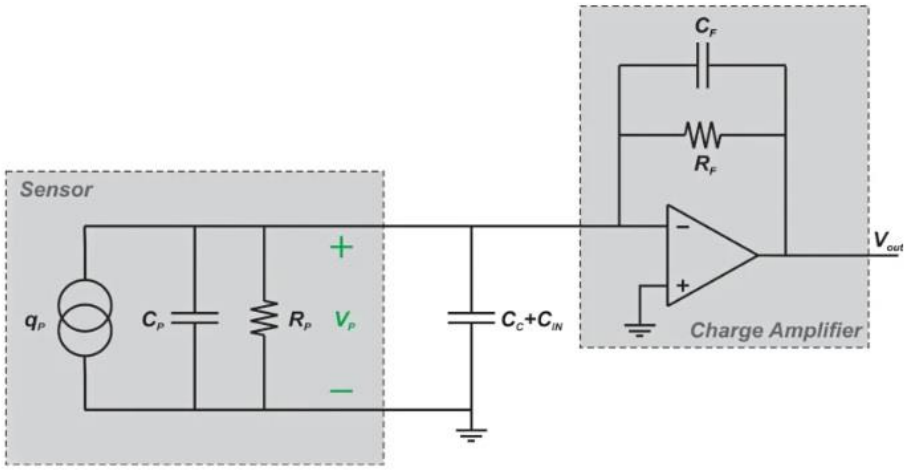

Figure 7. Charge amplifier circuit within a sensor[31]

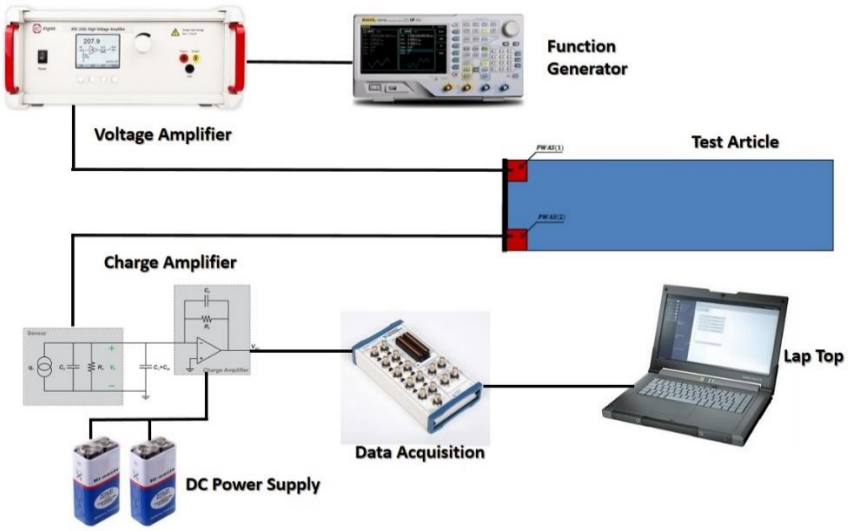

Figure 8. The schematic of the experimental setup

5.Results and discussion

As shown in table (4) the highest effective mass percentage is demonstrated at 1st bending mode (50.6% in the Z direction, and 95% rotation about Y) and the 1st torsion mode (15.2% rotation about X). It is worth noting that the 3rd mode has a high effective mass percentage (16.1% in the Z direction, 11.9% rotation about X, and 3.2% rotation about Y), as do some other modes (4th, 6th, and 9th), but the comparison of these values to those achieved by 1st and 2nd modes shows that those modes (1st &2nd) are sufficient to introduce the dynamic response for general bending and torsion modes, especially when computational and clear sampling efforts are taken into consideration. So, only first two modes will be accounted for in the FEM update process. As illustrated in the previous section, the excitation process is carried out to cover the designated frequency range of first two frequencies. Experimental frequency response function (FRF) is estimated based on the recorded sensor response using LabView software. FRF is then plotted in figure 9, the designated modes are found to be 16.49 and 104.95 Hz, respectively in addition to obvious noise nearly at 50 Hz. Numerical parameters correlation analysis is carried out using design exploration parameters correlation offered by ANSYS 22R1 software to select the significant material parameters to be updated in order to save the computational effort, where Pearson correlation is utilized with the number of samples and size of the generated set of 100 for each. Figure 10 shows that the most significant optimization parameters are Young's modulus in the X and Y directions (E_x&E_y) in addition to the Poisson ratio in the YZ direction (ν_{yz}) and the shear modulus in the XY direction (G_{xy}).

FEM is updated using the multi-objective genetic algorithm (MOGA) offered by ANSYS 22R1 software, where the MOGA technique is a controlled elitism variation of the popular NSGA (Non-dominated Sorted Genetic Algorithm). It accommodates numerous objectives and restrictions and seeks the global optimum [25]. The initial samples are set to be 100, and population to be iterated are 50 per generation for a maximum number of generations not more than 20, maximum allowable Pareto and convergence stability percentages are set to be 70% and 2%, respectively. Table (5) shows the results of the updated FEM parameters compared with initial FEM input parameters after convergence is achieved after 375 design points of iterations. The updated FEM is compared to both experimental measures and the initial FEM to show the variance between the estimated initial error and the final error of the updated FEM, as illustrated in table (6).

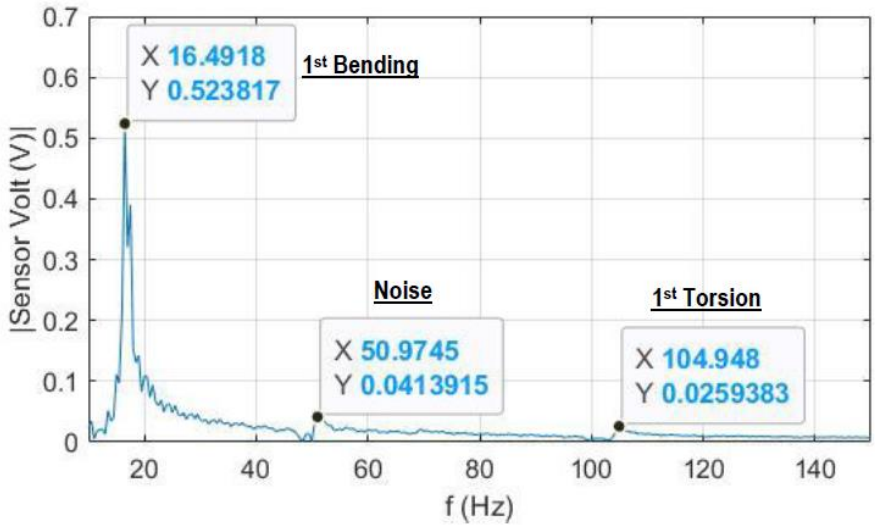

Figure 9. Frequency response function of the 1st bending & 1st torsion modes

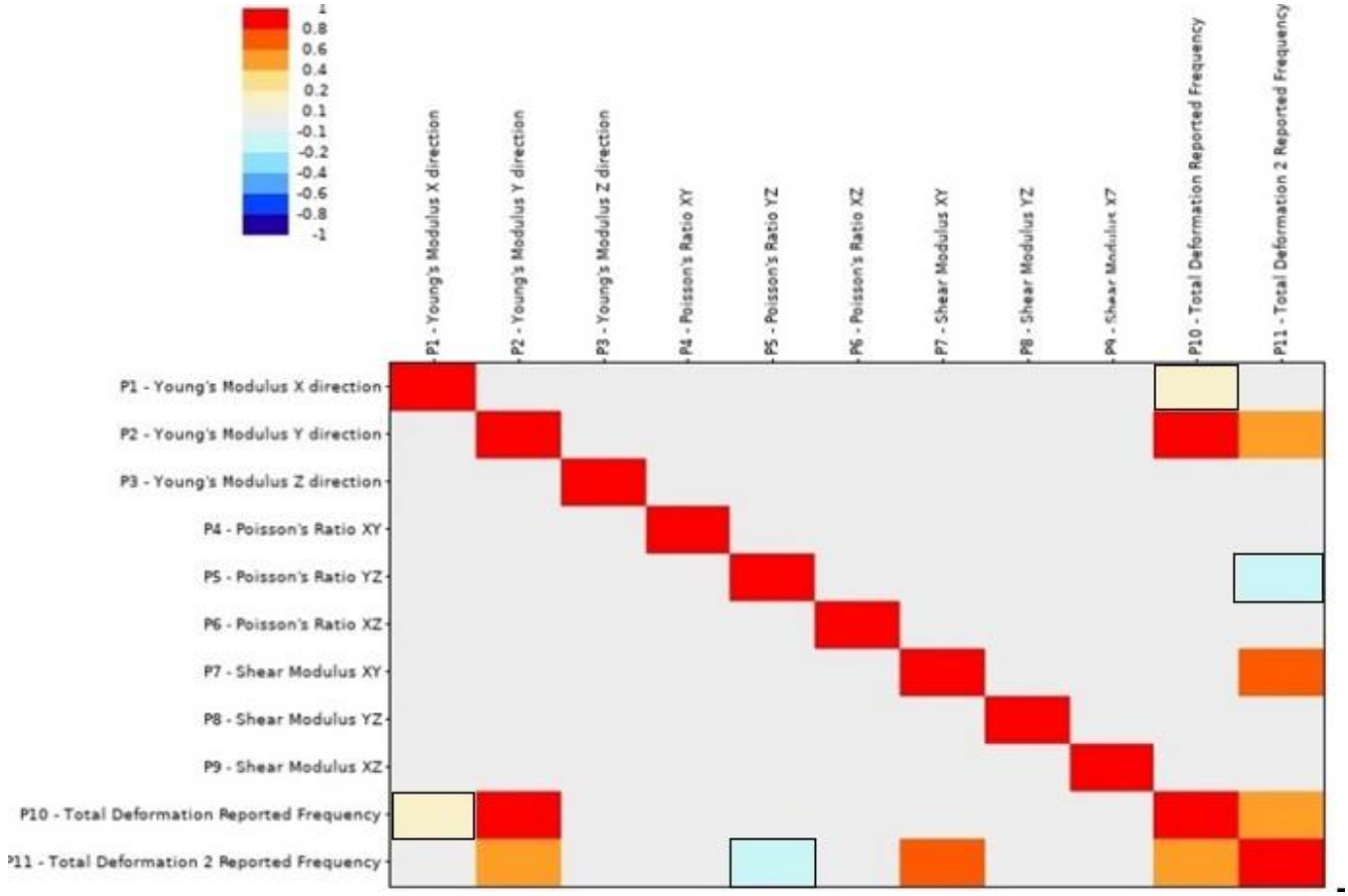

Figure 10. Linear correlation matrix of the target frequencies and material parameters

Table 5 comparison between initial and updated FEM parameters

Parameter	Initial FEM	Updated FEM
E_x	59.16 GPa	24.5 GPa
E_y	59.16 GPa	33.07 GPa
E_z	7.5 GPa	7.5 GPa
ν_{xy}	0.04	0.04
ν_{xz}	0.3	0.3
ν_{yz}	0.3	0.24
G_{xy}	17.5 GPa	34.57 GPa
G_{xz}	2.7 GPa	2.7 GPa
G_{yz}	2.7 GPa	2.7 GPa

Table 6 Comparison between estimated error before and after FEM updating.

NO.	Mode	Initial FEM	Experimental Measures	Error	Updated FEM	Error
1	1st bending	22.63	16.49	27.13%	16.8	1.9%
2	1st torsion	139.55	104.95	24.79%	104.85	0.1%

6.Coclusion

In this paper, piezoelectric ceramics are shown to be capable tools for carrying out some additional structural tasks such as model update via attaching a permanent, tiny, and cheap piece of equipment that can serve as actuator and/or sensor to a smart woven carbon fiber epoxy composite cantilever.

The shown test article is equipped with two APC 850 piezo-ceramics, one of which is assigned to be an actuator that is stimulated over the desired frequency range using allowable voltage to avoid depolarization due to the voltage limit of the used piezo-material, while the other is employed as a sensor where a simple charge amplifier is used to magnify the induced signal before being processed to extract natural modes from the measured FRF. The both sensor and actuator locations are selected to show the maximum actuating and response for the first initial natural modes.

First bending and first torsion modes are selected as the FEM updating target where the most significant effective masses are exhibited. Sensitivity analysis is carried out to reduce the number of optimization parameters by avoiding ineffective material parameters. The genetic optimization process determines most adequate material parameters that can cause the FEM to achieve the target frequencies.

Finally, the modal parameters of the investigated smart beam were re-estimated utilizing the updated material parameters. This FEM update reduced the maximum error from 27.13% and 24.79% to 1.9% and 0.1% respectively.

Refrences

[1] Anderson G L, Crowson A, and Chandra J 1992 Introuduction to smart structures *Inellegent structural systems* ed Tzou H Z and Anderson L (Netherlands: Kluwer Academic Publishers).
[2] Sinapius J M 2020 Introduction *Adaptronics – Smart Structures and Materials*, ed Sinapius J M (Berlin :Springer).
[3] Shivashankar P and Gopalakrishnan S 2020 Review on the use of piezoelectric materials for active vibration, noise, and flow control *Smart materials and structures* **29** 053001.
[4] Worden K, Bullough W A and Haywood J 2003 *Smart technologies* (London: World Scientific).
[5] Zorić N D, Simonovic´A M, Mitrovic Z S and Stupar S N 2013 Optimal vibration control of smart composite beams with optimal size and location of piezoelectric sensing and actuation *Journal of Intelligent Material Systems and Structures* **24** 499.
[6] Song G, Sethi V, and Li H N 2006 Vibration control of civil structures using piezoceramic smart materials: A review *Engineering Structures* **28** 1513.
[7] Abreu G L, Conceição S M D, Jr V L, Brennan M J and Alves M T S 2012 System identification and active vibration control of a flexible structure *Journal of the Brazilian Society of Mechanical Sciences and Engineering*, **34** 386.
[8] Orszulik R R, and Shan J 2012 Active vibration control using genetic algorithm-based system identification and positive position feedback *Smart materials and structures* **21** 055002.
[9] Saad M S, Jamaluddin H, and Darus I Z M 2015 Active vibration control of a flexible beam using system identification and controller tuning by evolutionary algorithm *Journal of Vibration and Control* **21** 2027.
[10] Kassem M, Yang z, Wang Y G and Safwat E 2020 Active dynamic vibration absorber for flutter suppression *Journal of Sound and Vibration* **469** 115110.
[11] Sethi V and Song G 2005 Optimal vibration control of a model frame structure using piezoceramic sensors and actuators *Journal of Vibration and Control* **11** 671.
[12] Pu Y, Zhou H, and Meng Z 2019 Multi-channel adaptive active vibration control of piezoelectric smart plate with online secondary path modelling using PZT patches *Mechanical Systems and Signal Processing* **120** 166.
[13] Lin C Y and Jheng H W 2017 Active vibration suppression of a motor-driven piezoelectric smart structure using adaptive fuzzy sliding mode control and repetitive control A*pplied Sciences* **7** 240.
[14] Levin R and Lieven N 1998 Dynamic finite element model updating using simulated annealing and genetic algorithms *Mechanical systems and signal processing* **12** 91.
[15] Wang J, Wang C and Zhao J 2017 Frequency response function-based model updating using Kriging model *Mechanical Systems and Signal Processing* **87** 218.
[16] Mishra A K, Mohammed A and Chakraborty S 2018 Improved numerical modelling of fiber reinforced plastics I-beam from experimental modal testing and finite element model updating *Int. J. Acoust. Vib.* **23** 26.
[17] Mondal S and Chakraborty S 2016 Identification of in-plane and out-of-plane elastic parameters of orthotropic composite structures. *Proc. ICSV* **23** 10.
[18] Shah M A S A, Yunus M A, Rani M N A, Mirza W I I W I and Sani M S M 2021 An Improved Method for Dynamic Behaviour Prediction of Carbon Fibre Reinforced Epoxy (CFRE) using Finite Element Model Updating *Proc. IOP Conf. Mater. Sci. Eng.* **1041** 012064.
[19] Bahari A R, Yunus M A, Rani M N A, Mirza W I I W I, Shah M A S A and Yahya Z 2021 Finite element modelling and updating of a thin plate structure using normal mode analysis *Proc. IOP Conf. Mater. Sci. Eng.* **1062** 012059.

[20] Ming Z, Qintao G, Lin Y and Baoqiang Z 2019 Finite element model updating of jointed structure based on modal and strain frequency response function *Journal of Mechanical Science and Technology* **33** 4583.
[21] Omar R, Rani M N A, Yunus M A, Rusli M, Shah M A S A, Izhan W I and Mizra W I 2021 Improvement in the accuracy of the dynamic behaviour prediction of a bolted structure using a simplified finite element model and model updating *Proc. IOP Conf. Mater. Sci. Eng.* **1041** 012051.
[22] Inc. I.E.E.E. 1978 *IEEE Standard on Piezoelectricity* (New York: IEEE)
[23] Inc. I.E.E.E. 1987 *IEEE Standard on Piezoelectricity* (New York: IEEE)
[24] Ikeda T 1996 *Fundamentals of piezoelectricity* (New York: Oxford university press).
[25] Inc.200 Products Mechanical APDL Release 2022 *22R1 ANSYS* (Pennsylvania: ANSYS).
[26] APC international L. 2015 *Physical and Piezoelectric Properties of APC Materials* https://www.americanpiezo.com/apc-materials/physical-piezoelectric-properties.html.
[27] Salem M A M 2017 *Determination of structural integrity using advanced structural monitoring systems* (Cairo: Military Technical College) p 129.
[28] Makkonen T, Holappa A, Ella J and Salomea M M 2001 Finite element siImulation of thin-film composite BAW resonators *IEEE Transactions on Ultrasonics, Ferroelctrics and Frequency Controrl* **48** 1241.
[29] *Giurgiutiu V 2008 Structural health monitoring with piezoelectic wafer active sensors (Massachusetts: Elsevier).*
[30] LOCTITE EA 9462. 2015 *Structural epoxy adhesive* https://www.henkel-adhesives.com/sg/en/product/structural-adhesives/loctite_ea_9462.html.
[31] Arar S 2022 Processing a Piezoelectric Accelerometer Output Using a Charge Amplifier https://www.allaboutcircuits.com/technical-articles/processing-a-piezoelectric-accelerometer-output-using-a-charge-amplifier/.